Genome-Wide DNA Methylation Profile Reveals Potential Therapeutic Targets at the Late Stage of Knee Osteoarthritis

Hongyan Shen
The General Hospital of Western Theater Command
Jie Long
The General Hospital of Western Theater Command
Mingmei Zhang
The General Hospital of Western Theater Command
Xing Chen
The General Hospital of Weatern Theater Command
Tao Wang
The General Hospital of Western Theater Command
Qingyun Xie
The General Hospital of Western Theater Command
Meng Wei (weimengwm@sina.com)
The General Hospital of Western Theater Command

Research article

Keywords: Osteoarthritis, DNA methylation, Cartilage, Knee

Posted Date: May 12th, 2020

DOI: https://doi.org/10.21203/rs.3.rs-27526/v1

Abstract

Background: The aim of this study was to use the latest BeadChip technology to obtain a genome-wide DNA methylation profile for cartilage from patients with primary knee osteoarthritis (OA), providing the first comprehensive description of DNA methylation changes in advanced knee OA.

Methods: Cartilage tissues were taken from patients after total knee arthroplasty and were divided into eroded group and intact group according to the cartilage status. The genome-wide DNA methylation profile was obtained using the Infinium MethylationEPIC BeadChip kit, which enables the analysis of >850,000 CpG sites. Comparisons of the two groups were performed to identify differentially methylated (DM) probes (DMPs). Gene ontology (GO) and Kyoto Encyclopedia of Genes and Genomes (KEGG) pathway analyses were applied to the functional annotation clustering of the DM genes.

Results: There was significant differential methylation between the two groups, and a total of 16,776 DMPs covering approximately 6,700 genes were identified, 92% of which were hypomethylated. Functional enrichment results revealed that the DM genes were significantly enriched for the extracellular matrix (ECM) proteins, cell adhesion molecules (CAM) and proteins in some inflammatory response pathways, especially the PI3K/Akt signalling pathway. Six genes including RNF43, SEMA4D, F11R, PKN1, FLT-1 and PTPN11 may be the potential biomarkers for OA.

Conclusion: Our data demonstrate the epigenetic dysregulation of many genes and pathways in the late stage of knee OA that appear to be involved in potential aetiological mechanisms of OA. DM genes closely associated with OA may become targets for treatment and may open new avenues for further research in the field.

Introduction

Osteoarthritis (OA) is one of the most common chronic musculoskeletal diseases characterized by articular cartilage degeneration, reactive hyperplasia of the joint edge and subchondral bone and eventually leads to joint pain, stiffness, deformity and joint function loss(1). Since OA likely occurs in the lower limb joints, OA has become a major cause of lower limb disability in the elderly.

As this disease attracts increasing attention from researchers, OA is no longer considered to be the result of mere mechanical stimulation but is believed to be caused by complex interactions between genetic and environmental factors(2). Age, gender, obesity, and genetics are recognized as major risk factors for OA. At present, the aetiology of OA has not been fully elucidated, and epigenetic alterations in chondrocytes are also key to the pathogenesis of OA(3). DNA methylation of CpG sites is the most widely studied in complex diseases during epigenetic modifications. Cartilage is composed of a single cell type (chondrocytes) and the extracellular matrix (ECM). ECM plays an important role in maintaining cartilage homeostasis, and its dysfunction is closely related to the pathogenesis of OA(4).

A series of candidate gene studies have demonstrated that the demethylation of specific promoters or enhancer regions of the matrix metalloproteinase (MMP3, MMP9, MMP13), ADAMTS-4, SOX-9, PH domain leucine-rich repeat protein phosphatase 1 (PHLPP1), and interleukin-8 (IL-8) genes causes self-expression changes related to OA chondrocytes(5–8). Subsequently, genome-wide DNA methylation assays for hip or knee cartilage have been reported, revealing differentially methylated (DM) genes or pathways associated with OA(9–12). These studies suggested that the methylation statuses of hip and knee cartilage were not identical, and the changes in DNA methylation occurred at the late sta ge of OA.

We found that the existing OA-related genome-wide DNA methylation studies were few, and their quality was varied. At present, a higher-throughput methylated BeadChip technology is gradually being applied (13). The Infinium MethylationEPIC BeadChip (EPIC) method has increased the number of detected CpG sites to more than 850,000. More extensive coverage and more mature data analysis make it the most suitable DNA methylation detection method for epigenetic genome-wide association analysis. Considering the importance of DNA methylation in the pathogenesis of OA and the fact that cartilage tissue comprises a single cell type, we selected knee OA cartilage as an ideal methylation research object on the basis of previous studies and collected paired samples. EPIC analysis was then performed to study the DNA methylation characteristics of advanced OA to obtain the DNA methylation profile and help to elucidate the pathogenesis of OA and identify new therapeutic targets.

Materials And Methods

Knee joint cartilage

Human cartilage tissues were collected from the knee joints of 8 patients undergoing knee arthroplasty because of the end-stage primary knee OA at the General Hospital of Western Theatre Command PLA (Chengdu, China) (6 females and 2 males; mean age (standard deviation, SD) = 63.38(7.46), range = 54 ~ 72). The diagnosis of OA was based on the criteria of the American College of Rheumatology, and all patients were screened to exclude OA due to trauma or other pathological conditions. The cartilage obtained from the tibial plateau and femoral condyles was divided into two groups for this study: (a) the outer region of the lateral tibial plateau and lateral femoral condyles (intact group) with an intact smooth cartilage surface and (b) the inner region of the medial tibial plateau and medial femoral condyles (eroded group) with visible loss of articular cartilage. Previous research has shown that methylation alterations occurred in the late stage (obviously eroded cartilage) but not in the intermediate stage of knee OA. The samples gathered were immediately stored at -80 °C. The local ethics committees approved this study, and informed consent was obtained from each patient who enrolled in the study.

DNA extraction and bisulfite treatment

Up to 200 mg cartilage tissue from each sample was ground into powder with liquid nitrogen. Following complete digestion in the lysis buffer, the phenol-chloroform method was employed to separate the DNA

into the aqueous phase. Then, the DNA was extracted after precipitation and washing. DNA quality and quantity were determined by agarose gel electrophoresis and a Nanodrop Spectrophotometer. A total of 2 µg of DNA was then subjected to bisulfite conversion using the EZ DNA Methylation kit (Zymo Research).

DNA methylation profiling

Genome-wide DNA methylation profiling was assessed using the Infinium MethylationEPIC BeadChip kit (Illumina), which analyses the methylation status of more than 850,000 methylation sites, covering 99% CpG islands of RefSeq genes, ENCODE open chromatin and transcription factor binding site regions, and FANTOM5 enhancer regions. Briefly, the bisulfite-converted DNA is amplified, fragmented and hybridized to the arrays. For each CpG site, methylation levels are measured by two types of design probes (type I and type II) attached to beads that maximize the detection range. Due to the different fluorescent labels used for the T (unmethylated) or C (methylated) alleles, the intensities of the unmethylated and methylated bead types are measured.

Data processing and statistical analysis

The raw data were extracted using R packages ChAMP(14) (version 2.8.9; https://bioconductor.org/packages/release/bioc/html/ChAMP.html). DNA methylation values are described as beta values (β), $\beta = M/(M + U)$, where M represents the fluorescent signal of the methylation probe and U represents the methylation signal of the unmethylated probe. The values range from 0 (no methylation) to 1 (100% methylation). For the quality control, default settings with filterXY set to false in the ChAMP package was used to filter probes. CpG probes with detection p-values above 0.01 and those located in sex chromosomes and at SNPs were filtered out from further analysis. To eliminate the difference caused by two type design probes and ensure the comparability of signal strength among samples, the beta-mixture quantile normalization (BMIQ) method was used to normalize the raw methylation level data. Singular value decomposition was then used to correlate principal components with biological and technical factors to decide if there are batch effects or confounding factors that need to be adjusted.

We then used the limma function within ChAMP to calculate differentially methylated probes (DMPs) at default settings, which supports calculating pairwise DMP between each pair of them. Adjusted P values were calculated by the Benjamini-Hochberg method for false discovery rate (FDR) control. To minimize false positives, significant DMPs were defined as those matching the following two requirements: (1) FDR-corrected P value < 0.05 and (2) at least 10% methylation difference (mean $|\Delta\beta| > 0.1$). Hierarchical clustering and principal components analysis (PCA) were performed based on the methylation of samples.

Enrichment analysis

According to identified DMPs, ClusterProfiler(15) (https://github.com/GuangchuangYu/clusterProfiler) was used for Gene Ontology (GO, http://www.geneontology.org/) and Kyoto Encyclopedia of Genes and Genomes (KEGG) enrichment analyses to identify functional annotations. Enriched GO and KEGG terms with FDR-corrected P values of less than 0.05 were reported. GO is an international standard classification system for gene function, and KEGG is the main public database of the classic pathway for experimental validation. GO enrichment analysis, based on the distribution and enrichment of genes, helps to clarify the differences among experimental samples at the level of gene function, which is mainly annotated from three categories: biological process (BP), cellular component (CC) and molecular function (MF). It is possible to employ KEGG pathway significant enrichment analysis to determine the specific gene sets mainly involved in the biochemical, metabolic and signal transduction pathways.

Results

Analysis of methylation profiling

A total of 731,845 probes were available for the subsequent analysis after quality control. Methylation was expressed as β values and can be simply interpreted as the percentage of methylation. Then, a total of 16,776 DMPs covering approximately 6,700 genes were identified from two groups of comparisons (FDR-corrected $P < 0.05$, mean $|\Delta\beta| > 0.1$) (Fig. 1a); of these DMPs, 92% were hypomethylated and the remainder showed hypermethylation (Fig. 1b). The eroded cartilage exhibited a higher degree of hypomethylation. Several examples of the methylation β value plot for a single probe are shown in Fig. 1c. The top 20 CpGs showing the largest differences in methylation levels are listed in Table 1. According to the functional genomic distribution, the majority (39%) were located in gene bodies as well as intergenic region, 8% were located in 5'UTR, 2% were located in 3'UTR, 1% were located in the first exon, and 10% were located within 1,500 bp upstream of the transcription start site(Fig. 1d). In the CpG island analysis, 2% belonged to CpG island, 13% belonged to shore area, 7% belonged to shelf area, and the remaining 78% belonged to open sea area (Fig. 1e). Meanwhile, more sites were noted in the N-shore regions of CpG island among hypomethylated CpGs (80%), and the proportion of sites noted in island region among hypomethylated CpGs was 10 times lower than that of hypermethylated CpGs (11%). All the differences suggested various ways in which DNA methylation modification affected the development of OA. Furthermore, we also performed a significant test of the degree of differentially methylated regions (DMRs) between the two groups with a maximum length of 300 bp. HOXA11-AS and HOXA-AS3 were the most significant DMR genes.

Illumina CpG ID	Associated gene	Location group	Island group	P-value	FDR-P value	△β
Hypermethylated						
cg03112105	LINC02017	IGR	opensea	2.26E-07	0.000171	0.397315
cg24487117	LINC02505	IGR	opensea	1.29E-10	1.82E-06	0.372313
cg23976004	LINC01568	IGR	opensea	1.75E-09	8.63E-06	0.371644
cg13954161	DLGAP2	IGR	shore	9.22E-06	0.001439	0.366826
cg12165219	DLGAP2	IGR	shore	4.7E-06	0.001	0.366255
cg18463993	TMEM97	Body	opensea	2.55E-10	3.17E-06	0.364534
cg06254440	LHX2	Body	island	2.01E-08	3.97E-05	0.360802
cg15539318	LINC02488	IGR	opensea	2.44E-07	0.000179	0.355454
cg10160614	LINC01107	IGR	shelf	1.81E-08	3.75E-05	0.354783
cg03232695	C5orf64-AS1	IGR	opensea	7.15E-11	1.34E-06	0.354736
cg03763796	VPREB1	TSS200	opensea	7.45E-10	5.56E-06	0.346046
cg20736310	KIF16B	IGR	opensea	1.2E-06	0.000452	0.343478
cg07937810	BCAS3	Body	opensea	2.21E-11	7.7E-07	0.34157
cg25921543	FHIT	Body	opensea	1.99E-08	3.96E-05	0.333673
cg06439547	COG2	Body	shore	3.4E-10	3.46E-06	0.332676
cg25898232	LOC102724152	IGR	opensea	5.8E-05	0.003935	0.331309
cg11673566	VPREB1	TSS1500	opensea	4.71E-13	8.25E-08	0.325432
cg01284527	VPREB1	TSS200	opensea	9.65E-11	1.53E-06	0.323087
cg09952002	HOXB3	5'UTR	shore	3.71E-08	5.88E-05	0.322487

Illumina CpG ID	Associated gene	Location group	Island group	P-value	FDR-P value	△β
cg02514003	SNTG2	IGR	opensea	1.89E-11	6.92E-07	-0.31922
Hypomethylated						
cg03288347	SEMA4D	IGR	opensea	9.25E-10	6.27E-06	-0.58807
cg11825199	GRIA4	Body	opensea	1.46E-13	5.36E-08	-0.56574
cg20946074	DMGDH	Body	opensea	7.54E-12	4.6E-07	-0.47618
cg01044101	RNLS	Body	opensea	1.47E-08	3.31E-05	-0.47522
cg24764730	KLHL12	Body	opensea	4.98E-11	1.24E-06	-0.47416
cg17776382	LINC01192	Body	opensea	8.75E-10	6.1E-06	-0.44696
cg08193273	TRHR	Body	opensea	6.57E-11	1.32E-06	-0.43989
cg12818596	SIX1	IGR	shelf	1.55E-07	0.000141	-0.43063
cg14427776	SVEP1	IGR	opensea	8.57E-09	2.29E-05	-0.4261
cg17222143	USH2A	Body	opensea	1.04E-10	1.61E-06	-0.42102
cg23559228	HOXA11-AS	Body	shore	1.14E-06	0.000441	-0.41828
cg15425541	SIX1	IGR	shelf	9E-07	0.000387	-0.41809
cg20994254	HOXA11-AS	Body	shore	3.53E-06	0.000843	-0.41719
cg24705380	FRS2	3'UTR	opensea	1.5E-08	3.32E-05	-0.41332
cg05467090	LINC02267	IGR	opensea	2.92E-09	1.17E-05	-0.40219
cg08866695	ACACB	Body	shelf	3.24E-10	3.46E-06	-0.40183
cg17612681	SPRED2	IGR	opensea	1.1E-08	2.76E-05	-0.40124

Illumina CpG ID	Associated gene	Location group	Island group	P-value	FDR-P value	△β
cg19276186	FAM167A-AS1	Body	opensea	9.13E-11	1.48E-06	-0.39502
cg26389913	NEDD1	IGR	opensea	2.1E-09	9.22E-06	-0.39472
cg03819089	SPRED2	IGR	opensea	7.69E-09	2.12E-05	-0.39313

Gene region: Annovar annotated location of gene region; Location group: ChAMP package auto-annotated probe location of gene region; IGR: intergenic region; TSS200: within 200 bp of transcription start site; 5'UTR: 5'-untranslated region; Island group: ChAMP package auto-annotated CpG island; FDR-P value: false discovery rate controlled P-value; △β: difference in methylation value between sample groups (eroded-intact).

Table 1

Top 20 significant hyper- and hypo-methylated CpGs in eroded compared to intact cartilage

Significant differential methylation between eroded and intact OA cartilage

We used hierarchical clustering and principal components analysis to classify the two groups in the study. Although the sample size and the classification were not optimal, some trends observed were meaningful. As shown in Fig. 2a, the two main clusters are obvious. The first cluster included only 6 eroded group specimens, and the other cluster included 2 eroded group specimens and 8 intact group specimens; among these specimens, the two eroded group specimens were also clustered separately. PCA of the samples confirmed this clustering (Fig. 2b). A clear separation between two groups is evident according to the different coordinate positions. The intact group was almost completely located in the first quadrant area, while the eroded group was mostly concentrated in the third quadrant. Both methods reflected the differences between groups of samples, providing a basis for the reliability of data analysis

Functional annotation of the differentially methylated genes

The annotation clustering was conducted for the DM genes. According to GO (Fig. 3a), the DM genes were mostly enriched in extracellular matrix (ECM) organization, positive regulation of cell adhesion and extracellular structure organization in BP. Cell adhesion, ECM and collagen were notably enriched in CC. In MF, cell adhesion molecule (CAM) binding was the most significant, and there were enrichments in cadherin binding, transcription factor activity, and RNA polymerase II proximal promoter sequence-specific DNA binding, which suggests a regulatory effect on transcription. The bubble chart (Fig. 3b) showed the relevant signalling pathways suggested by KEGG, among which the PI3K/Akt signalling pathway, Rap1 signalling pathway, phospholipase D signalling pathway, focal adhesion, and ECM-receptor interaction were meaningful.

Discussion

In this study, we examined the methylation profiles of chondrocytes from two regions of 8 primary OA knee joints. To overcome the limitations of small sample size and obtain more comprehensive methylation information, we performed the first genome-wide DNA methylation analysis by Illumina Human Methylation 850K BeadChip(13). In light of the results, several worthwhile findings were revealed. First, we found that the methylation profile that we obtained not only confirmed most of the known DM genes in OA but that more DM genes were detected for the first time, some of which were intimately involved in OA. These results indicate that epigenetic dysregulation plays a remarkable role in pathogenesis. Then, the results of GO and KEGG enrichment analysis suggested that the dysregulation of some of these genes disturbed the functions of ECM, and some of the genes participated in the inflammation of OA through signalling pathways.

Compared to previous studies such as 450K beadchip, many of the identified DM genes, such as GDF6, BMP6, SMAD3, ABI3BP, FZD1, MSX2, CHSY1 and MATN2(16–21), also appear in our methylation profile. Homeobox (hox) genes, known OA related DM genes, were also observed in our study; these genes include HOXB3, HOXB1, HOXBAS1, HOXA11-AS, and HOXA-AS3. Hox genes, which represent self-renewal capacity, encode transcription factors that regulate skeletal formation during development(22). A previous study(23) showed that discovering the regulatory mechanisms of Hox genes could not only help to elucidate the pathology and initiation of OA but also provide information for identifying biomarkers that reflect the early stage of OA. At the same time, the expression changes of Hox genes indicated the self-renewal capability of chondrocytes in the late stage of OA(12).

More importantly, some new DM genes that could lead to the progression of the disease were found in our study. RNF43 was one of the most hypermethylated genes. RNF43 plays an important role in the regulation of the Wnt/β-catenin pathway(24). Loss of function of RNF43 results in enhancement of the Wnt/β-catenin signalling pathway because of the decrease/lack of degradation of Frizzled. Meanwhile, the canonical Wnt/β-catenin signalling pathway has been implicated in the pathogenesis of OA, and an increased capacity for Wnt/β-catenin signalling might contribute to cartilage loss(25). In other words, RNF43, one of the potential target genes of Wnt/β-catenin signalling, could reduce cartilage damage by limiting Wnt/β-catenin signalling, which was suppressed in OA. Therefore, we conclude that continuing to study the role of RNF43 may provide new clues for the treatment of OA. In hypomethylated genes, the expression of semaphorin 4D (SEMA4D) was also likely to be associated with OA. SEMA4D/CD100 has multiple roles in immune activation, bone metabolism, and neural development. Recent findings(26) revealed the associations between an elevated systemic soluble fragment of SEMA4D (sSEMA4D) levels and the severity of infectious and inflammatory diseases. A study of rheumatoid arthritis (RA) (27) showed that elevated baseline levels of SEMA4D in RA patients were associated with radiographic progression, suggesting that SEMA4D may be an active mediator of joint damage caused by RA. Another study(28) confirmed that sSEMA4D levels were elevated in the synovium of RA patients and promoted the expression of proinflammatory cytokines, such as interleukin-6 (IL-6) and tumour necrosis factor α (TNFα). The inhibition of arthritis by the anti-SEMA4D antibody was also demonstrated in mice with

collagen-induced arthritis (CIA). Since the same inflammatory cytokines are also involved in OA(29), whether we can use SEMA4D as a potential therapeutic target for OA requires further research to determine.

Enrichment terms highlighted by GO revealed that certain DM genes were related to the control of chondrogenesis, especially ECM molecules and CAM. TGFBR1 receptor of transforming growth factor-β (TGF-β), fibroblast growth factor (FGF), bone morphogenetic protein (BMP), nuclear transcription factor SOX9, runt-domain transcription factor (RUNX2) and MMPs are methylated genes related to the chondrogenesis (4), and have been confirmed in our methylation profile again. NID1, F11R, COL19A1, ITGAE, ITGB1, and EDIL3 were newly discovered from the DM genes. The ECM protein interacts with integrin to initiate intracellular signalling. For instance, EDIL3 stimulated osteoblast differentiation by increasing the expression of RUNX2 through α5β1 integrin(30). This gene was also found to be a susceptibility locus for ankylosing spondylitis in a genome-wide association study in a Han Chinese population(31). Junctional adhesion molecule 1 (JAM1/JAM-A/F11R), a kind of CAM, was hypomethylated in OA, which is involved in leukocyte adhesion and migration, and its knockdown decreased cell-matrix adhesion and Rap1 activity(32). Research has shown that F11R mRNA is highly expressed in peripheral blood mononuclear cells (PBMCs) of RA patients and speculated that the F11R promoter − 688 C may be a protective factor for the development of anti-CCP antibodies(33). Coincidentally, another study of systemic lupus erythematosus revealed that the blockade of F11R might have therapeutic potential in patients with lupus(34). Since these diseases are all rheumatic diseases, these results lead us to speculate and investigate the roles that F11R and EDIL3 play in OA.

In this study, we examine the information provided by the enrichment of KEGG pathway. The PI3K/Akt signalling pathway, Rap1 signalling pathway, and phospholipase D signalling pathway are all connected with inflammatory factors. The PI3K/Akt signalling pathway is one of the most conspicuous terms involved in many diseases and is essential in regulating the pathophysiology of OA. As the PI3K/Akt pathway is a classic inflammatory signalling pathway, animal experiments have found that the inhibition of this pathway could attenuate the inflammatory response and was able to prevent aberrant bone formation(35). Several DM genes enriched in this pathway merit further study. PKN1 was hypermethylated in OA, but its role in OA has not been reported to date. PKN1 is a protein kinase whose catalytic domain is highly homologous to the protein kinase C (PKC) family. Tumour necrosis factor alpha (TNF-α) receptor-associated factors (TRAF) are the major mediators of transducing TNF signalling to a variety of functional targets, including activation of NF-κB, c-Jun NH2-terminal kinase (JNK), and apoptosis. PKN1 can silence NF-κB kinase (IKK) and JNK by phosphorylating TRAF1 and regulating the competitive binding between TRAF1 and TRAF2 to TNF receptor type 2 (TNFR2)(36, 37). PKN1, as a key factor that can directly interact with TNFR2, plays an important role in regulating the activity of NF-κB. In OA, hypermethylated PKN1 may be responsible for NF-κB activation after self-expression inhibition, or it may be the result of long-term stimulation of chronic inflammation, which requires further research to explain. At the same time, PKN1 inhibits Wnt/β-catenin signalling in a human melanoma cell research(38), suggesting that the role of PKN1 in the pathogenesis of OA should not be underestimated. FLT-1, vascular endothelial growth factor (VEGF) receptor 1, is a hypomethylated DM gene in this

pathway. Genome-wide studies have shown that VEGF is associated with OA, and increased expression of VEGF is positively associated with disease severity and pain. At present, the treatment of targeting VEGF to resist angiogenesis and enhance cartilage repair, particularly blocking or reducing FLT-1 expression, has been extensively studied in animal models of OA and RA(39, 40). Notably, supported by both the findings of a large number of studies and our genome-wide screening, this result points to the role of VEGF in the treatment of OA. We are looking forward to the development of a safer and more efficacious VEGF-targeted OA therapy in clinical practice.

Phospholipase D is a regulator of intercellular signalling and metabolic pathways, particularly in cells under stress conditions. Most studies have revealed the role of the phospholipase D signalling pathway in cancer, but the relationship between this protein and OA has not been determined(41). PTPN11 encodes the tyrosine phosphatase SHP-2; this hypomethylated DM gene, enriched in the phospholipase D pathway, may demonstrate its role in some aspects. PTPN11 was overexpressed in RA fibroblast-like synoviocytes (FLS) compared with OA FLS, and inhibition of SHP-2 in mice reduced RA FLS invasion, migration, and reduced arthritis severity, suggesting that targeting SHP-2 may be a therapeutic strategy for RA(42). Therefore, what is the role of SHP-2 in OA? The differential methylation of PTPN11 in our report suggests that we should reconsider whether the impact of OA disease status on research is neglected in RA studies with OA as a control and whether some of the effective treatment methods for RA are equally applicable to OA.

Conclusions

Our study represents the first comprehensive methylation profile of knee OA with the latest BeadChip technology and screened out a multitude of DM genes associated with OA. Some of the genes may be potential targets for treatment, such as RNF43, SEMA4D, F11R, PKN1, FLT-1 and PTPN11. However, this study does have limitations. The sample size is not large enough and we will subsequently perform gene expression and functional verification of the screened potential target genes. Fortunately, our study reduced the impact of unknown confounders and the contribution of unknown genetic variation compared to some previous methylation studies, which have used control tissue from disease-free body donors or patients undergoing surgery to correct knee fractures, such as the interference of osteoporosis caused by different ages. Finally, we hope that the same method for methylation detection can reach a consensus on data analysis standards to facilitate the integration of multiple studies in the future. Overall, the results of our study contribute to the understanding of pathogenesis in OA and help to identify the target pathways for OA therapy.

Declarations

Ethics approval and consent to participate:

The study was approved by the ethics committee of the General Hospital of Western Theater Command, and informed consent was obtained from the participants involved. All procedures performed in studies

involving human participants were compliant with the ethical standards of the Declaration of Helsinki. Informed consent was obtained from each patient who enrolled in this study.

Consent for publication:

All the authors approved the final version of the manuscript and agree to publication.

Availability of data and material:

The raw dataset obtained from Beadchip during the current study are not publicly available due to the follow-up experiments but are available from the corresponding author on reasonable request.

Competing interests:

The authors declare that they have no competing interests.

Funding:

The study was supproted by the Sichuan Provincial Science and Technology Department Foudation (grant nos.2018SZ0187, 2017SZ0128)Sichuan Provincial Cadre Health Care Foudation (grant no.2017-1302)

Author’s contribution:

M Wei, and Q Xie designed and supervised the study. H Shen performed experiments, analyzed data and wrote the manuscript. Q Xie provided clinical specimens. J Long, M Zhang and X Chen collected samples and clinical data. T Wang and M Wei critically reviewed and proofread the manuscript.

Acknowledgements:

The authors are very thankful to Genesky Biotechnologies Inc. (Shanghai, 201315) for its technical support. This study depended on the participation of the patients with knee osteoarthritis, to whom they are grateful.

References

1. Kean WF, Kean R, Buchanan WW. Osteoarthritis: symptoms, signs and source of pain. Inflammopharmacology. 2004;12(1):3-31.

2. O'Neill TW, McCabe PS, McBeth J. Update on the epidemiology, risk factors and disease outcomes of osteoarthritis. Best practice & research Clinical rheumatology. 2018;32(2):312-26.
3. Reynard LN, Loughlin J. Genetics and epigenetics of osteoarthritis. Maturitas. 2012;71(3):200-4.
4. Goldring MB, Tsuchimochi K, Ijiri K. The control of chondrogenesis. Journal of cellular biochemistry. 2006;97(1):33-44.
5. Roach HI, Yamada N, Cheung KS, Tilley S, Clarke NM, Oreffo RO, et al. Association between the abnormal expression of matrix-degrading enzymes by human osteoarthritic chondrocytes and demethylation of specific CpG sites in the promoter regions. Arthritis and rheumatism. 2005;52(10):3110-24.
6. Kim KI, Park YS, Im GI. Changes in the epigenetic status of the SOX-9 promoter in human osteoarthritic cartilage. Journal of bone and mineral research : the official journal of the American Society for Bone and Mineral Research. 2013;28(5):1050-60.
7. Bradley EW, Carpio LR, McGee-Lawrence ME, Castillejo Becerra C, Amanatullah DF, Ta LE, et al. Phlpp1 facilitates post-traumatic osteoarthritis and is induced by inflammation and promoter demethylation in human osteoarthritis. Osteoarthritis and cartilage. 2016;24(6):1021-8.
8. Takahashi A, de Andres MC, Hashimoto K, Itoi E, Oreffo RO. Epigenetic regulation of interleukin-8, an inflammatory chemokine, in osteoarthritis. Osteoarthritis and cartilage. 2015;23(11):1946-54.
9. Rushton MD, Reynard LN, Barter MJ, Refaie R, Rankin KS, Young DA, et al. Characterization of the cartilage DNA methylome in knee and hip osteoarthritis. Arthritis & rheumatology (Hoboken, NJ). 2014;66(9):2450-60.
10. Jeffries MA, Donica M, Baker LW, Stevenson ME, Annan AC, Humphrey MB, et al. Genome-wide DNA methylation study identifies significant epigenomic changes in osteoarthritic cartilage. Arthritis & rheumatology (Hoboken, NJ). 2014;66(10):2804-15.
11. Aref-Eshghi E, Zhang Y, Liu M, Harper PE, Martin G, Furey A, et al. Genome-wide DNA methylation study of hip and knee cartilage reveals embryonic organ and skeletal system morphogenesis as major pathways involved in osteoarthritis. BMC musculoskeletal disorders. 2015;16:287.
12. Zhang Y, Fukui N, Yahata M, Katsuragawa Y, Tashiro T, Ikegawa S, et al. Genome-wide DNA methylation profile implicates potential cartilage regeneration at the late stage of knee osteoarthritis. Osteoarthritis and cartilage. 2016;24(5):835-43.
13. Moran S, Arribas C, Esteller M. Validation of a DNA methylation microarray for 850,000 CpG sites of the human genome enriched in enhancer sequences. Epigenomics. 2016;8(3):389-99.
14. Tian Y, Morris TJ, Webster AP, Yang Z, Beck S, Feber A, et al. ChAMP: updated methylation analysis pipeline for Illumina BeadChips. Bioinformatics (Oxford, England). 2017;33(24):3982-4.
15. Yu G, Wang LG, Han Y, He QY. clusterProfiler: an R package for comparing biological themes among gene clusters. Omics : a journal of integrative biology. 2012;16(5):284-7.
16. Karlsson C, Dehne T, Lindahl A, Brittberg M, Pruss A, Sittinger M, et al. Genome-wide expression profiling reveals new candidate genes associated with osteoarthritis. Osteoarthritis and cartilage. 2010;18(4):581-92.

17. Zhang S, Peng J, Guo Y, Javidiparsijani S, Wang G, Wang Y, et al. Matrilin-2 is a widely distributed extracellular matrix protein and a potential biomarker in the early stage of osteoarthritis in articular cartilage. BioMed research international. 2014;2014:986127.
18. Su SL, Yang HY, Lee HS, Huang GS, Lee CH, Liu WS, et al. Gene-gene interactions between TGF-beta/Smad3 signalling pathway polymorphisms affect susceptibility to knee osteoarthritis. BMJ open. 2015;5(6):e007931.
19. van den Bosch MH, Blom AB, van de Loo FA, Koenders MI, Lafeber FP, van den Berg WB, et al. Brief Report: Induction of Matrix Metalloproteinase Expression by Synovial Wnt Signaling and Association With Disease Progression in Early Symptomatic Osteoarthritis. Arthritis & rheumatology (Hoboken, NJ). 2017;69(10):1978-83.
20. Chou CH, Lee CH, Lu LS, Song IW, Chuang HP, Kuo SY, et al. Direct assessment of articular cartilage and underlying subchondral bone reveals a progressive gene expression change in human osteoarthritic knees. Osteoarthritis and cartilage. 2013;21(3):450-61.
21. Chou CH, Lee MT, Song IW, Lu LS, Shen HC, Lee CH, et al. Insights into osteoarthritis progression revealed by analyses of both knee tibiofemoral compartments. Osteoarthritis and cartilage. 2015;23(4):571-80.
22. Seifert A, Werheid DF, Knapp SM, Tobiasch E. Role of Hox genes in stem cell differentiation. World journal of stem cells. 2015;7(3):583-95.
23. Pelttari K, Barbero A, Martin I. A potential role of homeobox transcription factors in osteoarthritis. Annals of translational medicine. 2015;3(17):254.
24. Tsukiyama T, Fukui A, Terai S, Fujioka Y, Shinada K, Takahashi H, et al. Molecular Role of RNF43 in Canonical and Noncanonical Wnt Signaling. Molecular and cellular biology. 2015;35(11):2007-23.
25. Corr M. Wnt-beta-catenin signaling in the pathogenesis of osteoarthritis. Nature clinical practice Rheumatology. 2008;4(10):550-6.
26. Maleki KT, Cornillet M, Bjorkstrom NK. Soluble SEMA4D/CD100: A novel immunoregulator in infectious and inflammatory diseases. Clinical immunology (Orlando, Fla). 2016;163:52-9.
27. Ha YJ, Han DW, Kim JH, Chung SW, Kang EH, Song YW, et al. Circulating Semaphorin 4D as a Marker for Predicting Radiographic Progression in Patients with Rheumatoid Arthritis. Disease markers. 2018;2018:2318386.
28. Yoshida Y, Ogata A, Kang S, Ebina K, Shi K, Nojima S, et al. Semaphorin 4D Contributes to Rheumatoid Arthritis by Inducing Inflammatory Cytokine Production: Pathogenic and Therapeutic Implications. Arthritis & rheumatology (Hoboken, NJ). 2015;67(6):1481-90.
29. Wojdasiewicz P, Poniatowski LA, Szukiewicz D. The role of inflammatory and anti-inflammatory cytokines in the pathogenesis of osteoarthritis. Mediators of inflammation. 2014;2014:561459.
30. Oh SH, Kim JW, Kim Y, Lee MN, Kook MS, Choi EY, et al. The extracellular matrix protein Edil3 stimulates osteoblast differentiation through the integrin alpha5beta1/ERK/Runx2 pathway. PloS one. 2017;12(11):e0188749.

31. Lin Z, Bei JX, Shen M, Li Q, Liao Z, Zhang Y, et al. A genome-wide association study in Han Chinese identifies new susceptibility loci for ankylosing spondylitis. Nature genetics. 2011;44(1):73-7.
32. Mandell KJ, Babbin BA, Nusrat A, Parkos CA. Junctional adhesion molecule 1 regulates epithelial cell morphology through effects on beta1 integrins and Rap1 activity. The Journal of biological chemistry. 2005;280(12):11665-74.
33. Fang TJ, Lin CH, Lin YZ, Li RN, Ou TT, Wu CC, et al. F11R mRNA expression and promoter polymorphisms in patients with rheumatoid arthritis. International journal of rheumatic diseases. 2016;19(2):127-33.
34. Tsou PS, Coit P, Kilian NC, Sawalha AH. EZH2 Modulates the DNA Methylome and Controls T Cell Adhesion Through Junctional Adhesion Molecule A in Lupus Patients. Arthritis & rheumatology (Hoboken, NJ). 2018;70(1):98-108.
35. Xue JF, Shi ZM, Zou J, Li XL. Inhibition of PI3K/AKT/mTOR signaling pathway promotes autophagy of articular chondrocytes and attenuates inflammatory response in rats with osteoarthritis. Biomedicine & pharmacotherapy = Biomedecine & pharmacotherapie. 2017;89:1252-61.
36. Kato T, Jr., Gotoh Y, Hoffmann A, Ono Y. Negative regulation of constitutive NF-kappaB and JNK signaling by PKN1-mediated phosphorylation of TRAF1. Genes to cells : devoted to molecular & cellular mechanisms. 2008;13(5):509-20.
37. Gotoh Y, Oishi K, Shibata H, Yamagiwa A, Isagawa T, Nishimura T, et al. Protein kinase PKN1 associates with TRAF2 and is involved in TRAF2-NF-kappaB signaling pathway. Biochemical and biophysical research communications. 2004;314(3):688-94.
38. James RG, Bosch KA, Kulikauskas RM, Yang PT, Robin NC, Toroni RA, et al. Protein kinase PKN1 represses Wnt/beta-catenin signaling in human melanoma cells. The Journal of biological chemistry. 2013;288(48):34658-70.
39. Nagao M, Hamilton JL, Kc R, Berendsen AD, Duan X, Cheong CW, et al. Vascular Endothelial Growth Factor in Cartilage Development and Osteoarthritis. Scientific reports. 2017;7(1):13027.
40. Hamilton JL, Nagao M, Levine BR, Chen D, Olsen BR, Im HJ. Targeting VEGF and Its Receptors for the Treatment of Osteoarthritis and Associated Pain. Journal of bone and mineral research : the official journal of the American Society for Bone and Mineral Research. 2016;31(5):911-24.
41. Bruntz RC, Lindsley CW, Brown HA. Phospholipase D signaling pathways and phosphatidic acid as therapeutic targets in cancer. Pharmacological reviews. 2014;66(4):1033-79.
42. Maeshima K, Stanford SM, Hammaker D, Sacchetti C, Zeng LF, Ai R, et al. Abnormal PTPN11 enhancer methylation promotes rheumatoid arthritis fibroblast-like synoviocyte aggressiveness and joint inflammation. JCI insight. 2016;1(7).

Figures

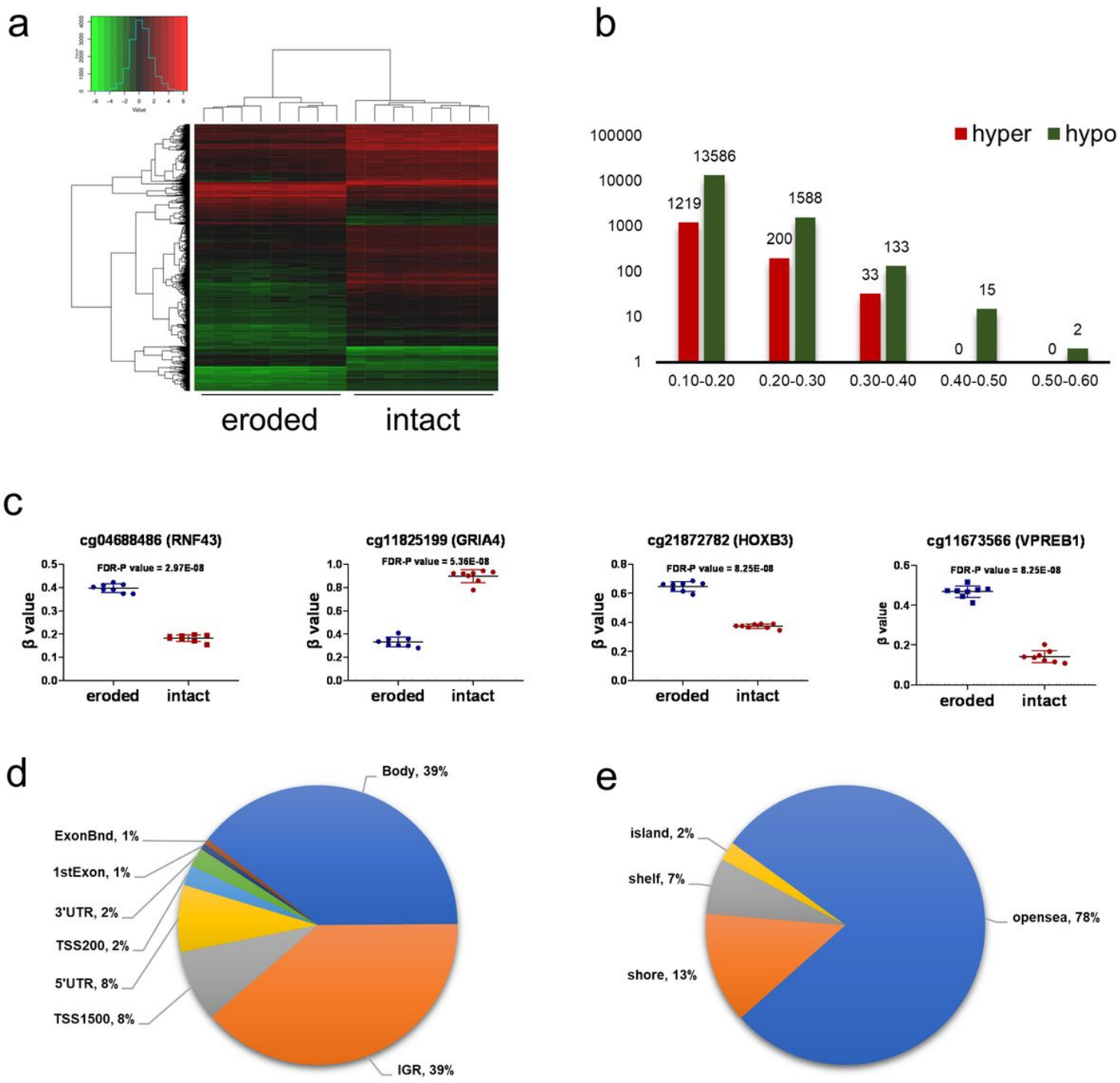

Figure 1

Genome-wide DNA methylation profile in knee OA chondrocytes. a Heatmap showing the variation of 16,776 significant DMPs identified in knee OA samples. Rows represent DMPs, and columns represent samples. The dendrograms at the top and left show clustering of samples and loci, respectively. Red indicates hypermethylation, and green indicates hypomethylation. The methylation scales are shown to the left of the heatmap. b Summary of the DMPs. The red bars represent hypermethylation, and the green bars represent hypomethylation. The Y-axis indicates the frequency of hyper- and hypomethylation (log scale). The frequency was marked at the end of each bar. The X-axis indicates the groups of |Δβ| values.

c Examples of β value plots selected from top DMPs. d Graph shows the percentage of DMPs according to their functional genomic distribution. e Graph shows the percentage of DMPs according to their CpG content and neighborhood context

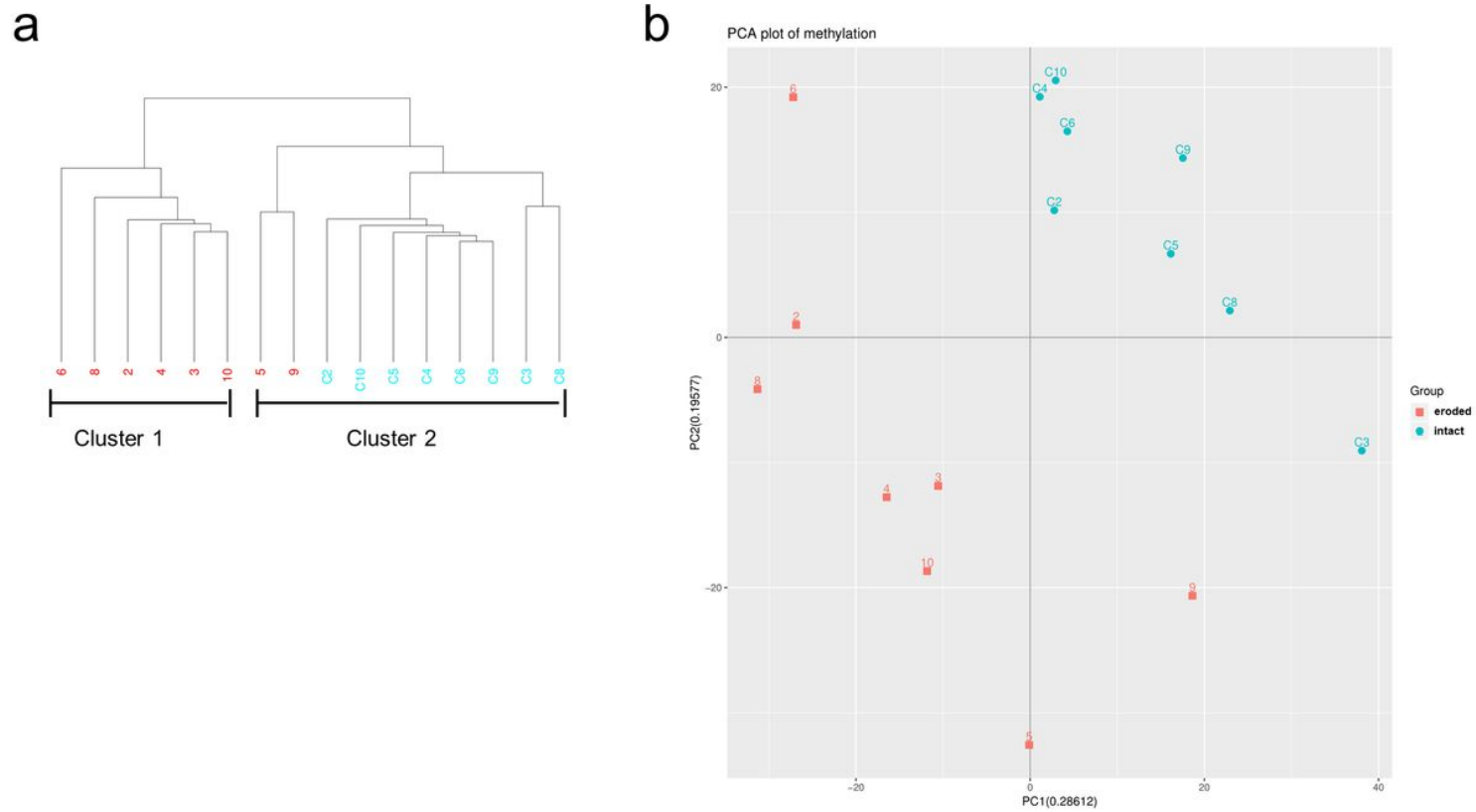

Figure 2

Comparison of methylation between two groups of samples. a Unsupervised hierarchical clustering of the β values in the samples reveals 2 distinct clusters. b PCA of β values in samples shows two distinct groups corresponding to those identified through unsupervised hierarchical clustering. The red squares represent eroded cartilage samples, while the blue circles represent intact cartilage samples

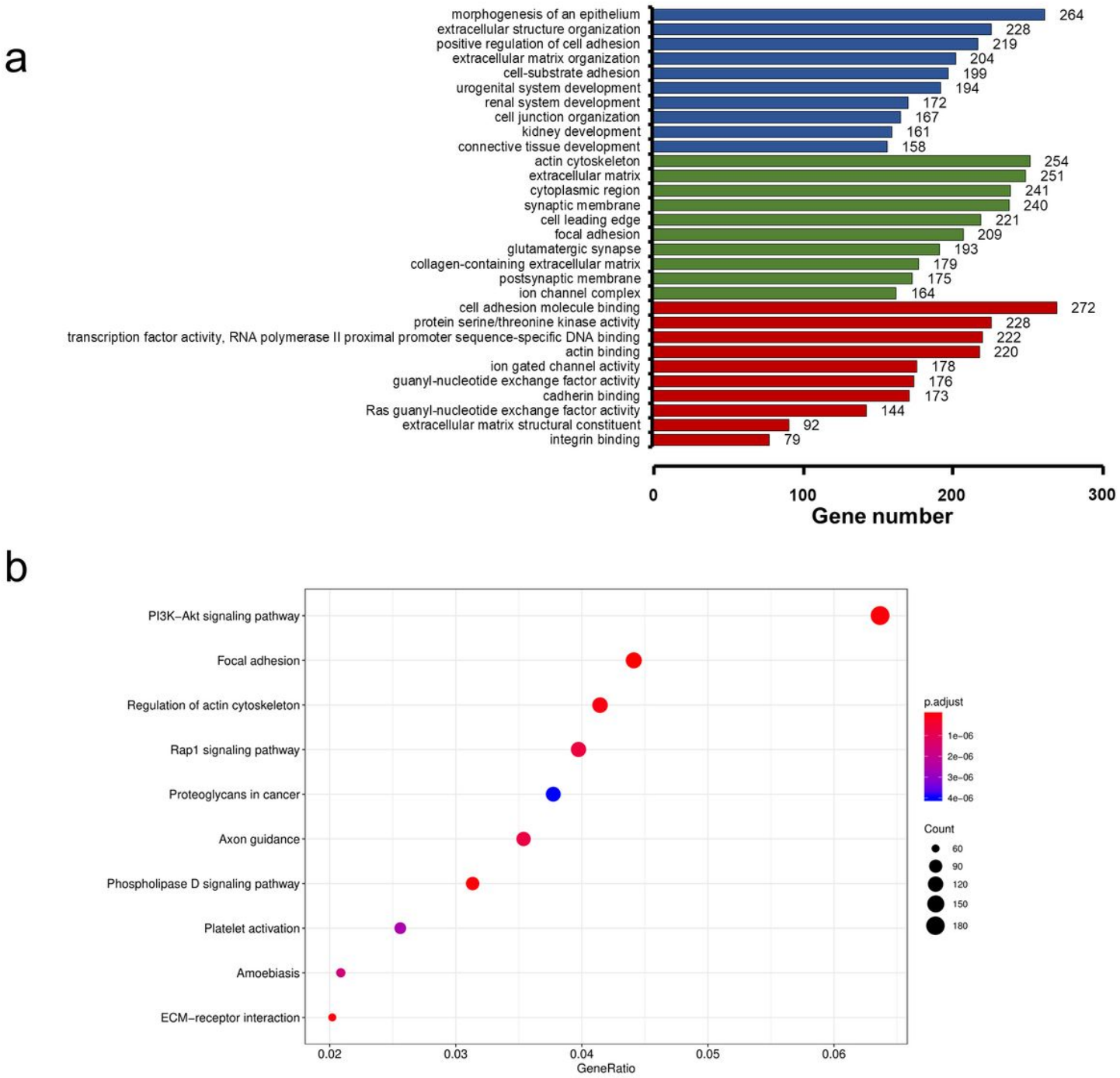

Figure 3

Gene Ontology terms and KEGG pathway enrichment of identified DM genes. a Gene ontology enrichment analysis of the 6,545 DM genes. P-values are Benjamini-corrected. The illustration shows the top ten terms in the three categories (BP, CC, and MF), and the p-values are all less than 0.001. Colours to distinguish categories. The number of genes enriched in each term was marked behind. b Top ten KEGG enrichments of 2,969 DM genes are shown. The gene ratio is shown along the X-axis, while the KEGG terms are shown along the Y-axis. The rich factor is the proportion of the number of DM genes enriched

for terms vs. the total number of DM genes that can be annotated with KEGG. The bubble indicates the number of genes matched in the KEGG pathway. The colour represents the adjusted p-value